JOURNAL OF MATERIALS SCIENCE: MATERIALS IN MEDICINE **10** (1999) 111–120

Role of interconnections in porous bioceramics on bone recolonization *in vitro* and *in vivo*

J. X. LU, B. FLAUTRE, K. ANSELME, P. HARDOUIN
Institut de Recherche sur les Maladies du Squelette (IRMS), Ru de Docteur Calot, 62608 Berck-Sur-Mer Cedex, France

A. GALLUR, M. DESCAMPS, B. THIERRY
Laboratoire des Matériaux Avances et Céramiques, Université de Valenciennes et du Hainaut-Cambrésis, Centre Régional d'Innovation et de Transfert Technologique ''Céramiques fines'', Zone industrielle du champ de l'abbesse, 59600 Maubeuge, France

The interconnections in a porous biomaterial are the pathways between the pores. They conduct cells and vessels between pores. Thus they favour bone ingrowth inside ceramics. The aim of our study was to determine the effect on bone ingrowth of interconnections in two ceramics: hydroxyapatite (HA) and β-tricalcium phosphate (β-TCP) with the same porosity of about 50% and a mean pores size of 100–300 μm and a mean interconnection size of 30–100 μm. *In vitro*, four discs for osteoblast culture were studied after 14 and 28 days of incubation. The results show that human osteoblasts can penetrate interconnections over 20 μm in size, and colonize and proliferate inside macropores, but the most favourable size is over 40 μm. *In vivo*, eight cylinders were implanted in the middle shaft of both rabbit femurs for 12 or 24 weeks. The histomorphometric results show that interconnections in porous ceramics favour bone ingrowth inside the macropores. In the HA group the rate of calcification and bone ingrowth do not differ, and chondroid tissue is observed inside pores. But in β-TCP, the calcification rate and the bone ingrowth increased significantly. At week 12 significant correlation between new bone ingrowth and the size of the interconnections is observed between new bone ingrowth and the density of pores. In conclusion we notice that *in vivo* a 20 μm interconnection size only allows cell penetration and chondroid tissue formation; however the size of the interconnections must be over 50 μm to favour new bone ingrowth inside the pores. We propose the concept of ''interconnection density'' which expresses the quantity of links between pores of porous materials. It assures cell proliferation and differentiation with blood circulation and extracellular liquid exchange. In resorbable materials, pore density and interconnection density are more important than their size, contrary to unresorbable materials in which the sizes and the densities are equally important.

1. Introduction

The physico-chemical composition of ceramics of calcium phosphate is similar to the mineral constituents of our skeleton. As far back as 1920, ceramics were used as bone substitute and showed the ability to be recolonized by bone tissue. Then, their use was abandoned. But since 1970, many studies have investigated their behaviour in biological fluids. They were considered biocompatible either *in vitro* or *in vivo* [1–4]. Meanwhile, a lot of factors influence the biological behaviour of calcium phosphate ceramics aside from their chemical composition, the pore size and macroporosity (pore size > 100 μm) have a direct influence on bone formation, but do not influence the biodegradation rate [5]. The studies have mainly investigated bone ingrowth inside pores, but a few studies have looked at interconnections related to new bone tissue. The interconnections are literally a pathway between pores to favour cellular and vascular penetration, which assures bone ingrowth inside pores. The aim of our study is to determine the link between interconnections and pores on cellular and bone tissue recolonization in porous materials.

2. Experimental procedure

2.1. Materials

Two bioceramics, hydroxyapatite (HA) and β-tricalcium phosphate (β-TCP) of the same porosity with an identical mean size of pores and interconnections were used (Table I).

TABLE I Physico-chemical characterization of bioceramics

	Porosity (%)[a]		Size (μm)[b]		Specific surface[a] (m^2 g)	Ratio Ca/P[c]
	Macro	Micro	Macropore	Interconnections		
HA	50	2.7	100–300	30–100	0.94	1.64 ± 0.03
β-TCP	52	4.2	100–300	30–100	4.00	1.55 ± 0.03

[a] Tested by mercury porosimetry.
[b] Morphometry.
[c] Inductive plasma coupling.

TABLE II Distribution of samples

		Time		Samples		Observation (*n*)			
		(h)	(weeks)	HA	β-TCP	TLM	SEM	CP	CS
In vitro	Osteoblasts	4	1, 2, 3, 4[a]	36	36	4	2	4	4
In vivo	Rabbits		0, 12, 24[b]	32	32	8	2		

[a] Two and four weeks for TLM and SEM.
[b] Four and eight weeks for preliminary study ($n = 1$).

For the *in vitro* study, discs of 13.2 mm diameter and 1.4 ± 0.2 mm height were sterilized by dry heat at 180 °C for 1 h (Table II). Control discs, 13 mm in diameter (Thermanox®, OSI) were also used. Osteoblast cells were obtained from cancellous bone tissue from the iliac crest of a six year-old child. These cells were seeded after a second passage. The culture medium was Dulbecco's Modified Eagle's Medium (Eurobio) with 2 mM of L-glutamine, 10% fetal calf serum, 50 UI ml^{-1} penicillin, 50 μg ml^{-1} streptomycin and 2.5 μg ml^{-1} mycostatin (Eurobio).

For the *in vivo* study, cylinders of 3 mm diameter and 6.1 ± 0.2 mm length were sterilized by γ-radiation at 25kGy (Table II).

White female New Zealand adult rabbits with a mean weight 4 kg (ranging from 3.7 to 4.3 kg) before implantation were included in the study. Rabbits were fed with standard rabbit chow pellets and tap water *ad libitum*.

2.2. Methods

2.2.1. In vitro study

Discs were soaked in the culture medium under vacuum. An osteoblast suspension was prepared with the culture medium to obtain 4×10^4 cells ml^{-1}. One millilitre of cell suspension was then inoculated on the discs in each well and for each kind of material. The medium was changed twice a week.

At 4 h and 7, 14, 21 and 31 days after incubation (37.0 ± 0.2 °C temperature, 5.0 ± 0.1% CO_2 and 98% humidity) cell proliferation and protein synthesis analysis were studied; histologic observations were made after 14 and 28 days.

In order to analyse cell proliferation (CP) and cellular protein synthesis (CS), cells were counted after 4 h and 7, 14, 21 and 31 days after incubation using a COULTER Z1 (Coultronics). After 21 days of culture, cells were collected, sonicated and alkaline phosphatase activity (ALP) was measured with an Enzyline Kit® for ALP (Cobas Mira, Biomerieux). Cells were rinsed with DMEM + 0.1% bovine serum albumin + 50 μg ml^{-1} ascorbic acid + 10^{-8} M K_2 vitamin. Then, the cells were treated with 1.25 (OH) $2D_3$ vitamin (10^{-8} M) or with the control solution (absolute ethanol). After 48 h of culture, media were collected and were used for osteocalcin measurement with a Lumitest Kit® Osteocalcin and for Type I procollagen with Procollagen-C Kit® (Hoechst-Behring).

Material for histological observation was evaluated by transmitted light microscopy (TLM) and scanning electronic microscopy (SEM). For TLM after 14 and 28 days of culture, the discs were fixed in a mixed solution (1 volume of 4% glutaraldehyde + 1 volume of 2% paraformaldehyde + 2 volumes of 0.2% monosodium dipotassium, NaK_2P) for 2 h. The samples were then dehydrated in graduated alcohol (85–100%, cleared with toluene before being embedded in polymethylmetacrylate. After hardening, the samples were cut perpendicular to the contact surface and then 150–200 μm thick sections were cut under water lubrication with a microtome Leitz 1600 saw (Microm). Microradiographs of 100 μm sections were performed with an OEG 50 Machlett tube (Bernas Medical). The sections were then polished automatically (Exakt) to a thickness of 50 μm and stained with May Grünwald Giemsa. For SEM after 14 and 28 days of culture, the specimens were twice rinsed in buffered sodium phosphate and then fixed in the mixed solution as described above for 30 min. The samples were rinsed for 2 h in buffered NaK_2P solution at 0.175% and dehydrated in graduated alcohol.

2.2.2. In vivo study

Under general anaesthesia, a surgical approach at the lateral side of the femur and a cavity 3 mm in diameter and 6 mm in depth in the middle shaft of the femur was performed with an electric drill and then manually. The bone debris was washed with saline solution.

Five rabbits with ten implants in each group (HA or β-TCP) were sacrificed by an overdose of sodium pentobarbital after zero, 12 and 24 weeks. One rabbit (one implant of HA and β-TCP) was sacrificed at four weeks and another eight weeks after implantation for a preliminary study. At two and 17 days before sacrifice, a double label of oxycycline (25 mg kg^{-1} Vibraveineuse®) and alizarine complexon 30 mg Kg^{-1}) was made.

For histological observation under TLM the femoral shafts were harvested, cleaned of soft tissues and fixed in 10% neutral buffered formalin, then rinsed in tap water for 12 h. Histological preparation of samples was the same as in the *in vitro* study. The 50 μm thick sections were finally stained with Picro-Fuschine Van Gieson.

For SEM examination, the samples were twice rinsed in buffered sodium phosphate and then fixed for one week. The preparation method was the same as in the *in vitro* study.

For histomorphometric evaluation, different histomorphometric parameters were measured on stained sections by linear intersect and point counting techniques using integrated eye pieces (KPL 16; Carl Zeiss) [16]. Distances were also measured with a micrometer. On the microradiograph, a semi-computerized image analysis method (Kontron) measured pore size, interconnections, volume of new bone formed inside pores and the residual biomaterial. The following were measured

1. The mineral apposition rate (MAR, is micrometres per d) is the distance between two consecutive labels divided by time between the labelling periods $\times 160$ magnification.

2. The new bone volume (NBV) and the residual material volume (RMV) express, respectively, the per cent of new bone tissue and residual material in the implant section $\times 128$ magnification, where the material degradation rate (MDR, per cent) is

$$\left(1 - \frac{\mathrm{RMV}t}{\mathrm{RMV}t_0}\right) \times 100\%$$

where RMV_t is the residual material volume at one time t and RMV_{t_0} is the residual material volume at the initial time, t_0.

3. The relative osteoid tissue volume (ROV) is the per cent of new bone volume occupied by osteoid tissue.

(NBV, RMV and ROV were measured manually in seven fields per each stained section. Two sections were prepared by specimen $\times 128$ magnification).

4. The proportion or depth of tissue penetration (PTP): The PTP for chondroid or bone tissue is measured by the distance (millimetres) from the edge of the section. Four measurements in one section were performed in four directions on x and y-axis ($\times 40$ magnification). Thus

$$\mathrm{PBTP}(\%) = \frac{\text{Mean depth of bone tissue penetration(mm)}}{\text{Mean radius (mm)}} \quad (9)$$

$$\mathrm{PCTP}(\%) = \frac{\text{Mean depth of chondroid tissue penetration(mm)}}{\text{Mean radius (mm)}}$$

5. The size (micrometres) and density (per millimetre square) of interconnections and pores. A manual method was used, with an eyepiece micrometer (magnification $\times 160$) on stained sections and a semiautomatic computerized method on the microradiograph (Vidas 21, Kontron) : two sections were measured per specimen.

The diameter of interconnections (IC) and the maximal diameter of the macropores (MP) were measured. The mean size and density of macropores and interconnections were calculated, as follows

Interconnection density(DsIC) = number of interconnections per section surface $(\mathrm{mm})^2$

Macropores density (DsMP) = number of macropores per section surface (mm^2)

Ratio of interconnections/macropores (IC/MP) = DsIC/DsMP

Statistically the results are expressed by the mean and the standard deviation (SD). The unpaired bilateral t-test (SYSTAT®) was used to compare the two group (HA and β-TCP) by delay at zero, 12 and 24 weeks). The significance was at 95% with $p < 0.05$. The correlation between the mean size of interconnections or macropores and DsMP or DsPC with the NBV was studied by the Pearson correlation coefficient, r, with a significance $p < 0.05$.

3. Results

3.1. *In vitro study*

In the *in vitro* study four samples were analysed for cellular protein synthesis, cell proliferation and TLM, and two samples by SEM. A total of 32 samples were used for each material and control category.

The results of cellular proliferation (cells/mm^2 have shown greater proliferation in HA than in β-TCP (Fig. 1). Cell proliferation and attachment in the two porous bioceramics were weaker than in the control group (attachment: 8.33 ± 1.89 cells/mm^2 for HA, 14.74 ± 4.43 cells/mm^2 for β-TCP and 129.52 ± 15.81 cells/mm^2 for the control). Analysis of the cell proliferation factor, i.e. the ratio of the number

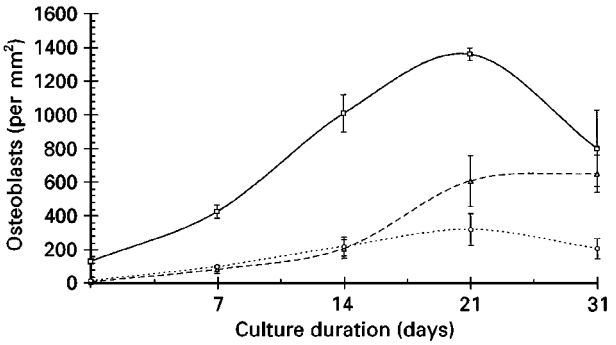

Figure 1 Human osteoblasts proliferation: (- - - -) HA, (· · · ·) TCP, (——) control. Initial harvest taken at 4 h.

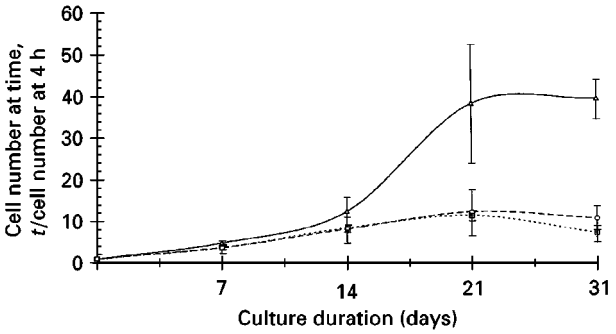

Figure 2 Cell proliferation factor: (——) HA, (- - - -) TCP, (· · · ·) control. Initial harvest taken at 4 h.

of cells at a time, t, to the number of cells attached at 4 h has shown an increase of the proliferation factor with time until 21 days of culture for all groups, then a decrease in the control and β-TCP or stabilization in HA (Fig. 2).

Osteoblastic activity of the cells was increased (Table III). With SEM, the cellular morphology is similar for both biomaterials. A cellular layer spreads on the surfaces of the materials evenly covering the opened macropores. On the broken surface of discs, osteoblasts are observed to colonize the macropores. After 28 days of culture their penetration is greater than at 14 days (Fig.3a, b). Some osteoblasts were observed in the interconnections (Fig. 3c, d). Nevertheless, no modification of the microstructure of either ceramics after culture was seen by SEM observation.

On stained sections in TLM, cellular penetration in time is deeper for the β-TCP group than for the HA group. After 28 days of culture the cellular penetration depth is only two rows of pores for the HA group, while three rows occur in the β-TCP group. After 14 days of culture, there are a few cells inside the pores (Fig. 4a, b).

The sizes of interconnections with cells vary from 19.15 to 215.43 μm (with a mean size of 78.67 ± 37.41 μm for the β-TCP group and 70.08 ± 38.76 μm for the HA group); 60 μm is the most frequent size of interconnections with cells in both groups after 28 days of culture (Fig. 5). On sections, for the same length of contact with cells (CS), the number of underlying interconnections with cells is greater for β-TCP (4.38 ± 0.87 passages cm^{-1}) than for HA (1.24 ± 0.41 passages cm^{-1}) after 28 days of culture (Fig. 4c).

3.2. *In vivo* study

In Table IV, the results show that MAR is higher in the bone adjacent to the implantation site than in both biomaterials ($p < 0.001$) and lower HA than β-TCP. In β-TCP, MAR increases significantly with time ($p < 0.001$) whereas no difference is observed with time in bone adjacent to the implantation site and in the HA group. In the β-TCP group, RMV decreases significantly with time ($p < 0.005$). In the HA group no difference is observed. At 12 weeks after implantation, NBV in both materials increased but was higher in β-TCP than in HA ($p < 0.001$). From 12 to 24 weeks after implantation, in β-TCP, the curve of the NBV remains stabilized and increases significantly with time ($p < 0.05$).

At eight weeks, in the β-TCP group, new bone formation grows towards the centre of the implant (Fig. 6a, b). In the HA group, bone ingrowth remains only at the periphery of the implant, a chondroid tissue is seen inside the implant (Fig. 6c, d) and increases significantly with time ($p < 0.05$) . The proportion of chondroid tissue (PCTP) compared with the depth bone tissue penetration (PBTP) increases significantly from 30 to 50% ($p < 0.05$).

The mean vascular diameter is about 20 μm, with a range of 10–40 μm for both bioceramics, but the vascularization in β-TCP is higher than that in HA.

On the microradiograph, the characterization of the microstructure of both materials was determined at zero weeks with a computerized image analyser. Neither the mean size of the interconnections and pores, nor the distribution of interconnections are different in both materials. But pore density, interconnections density and pore distribution are different between the two groups of biomaterials ($p < 0.05$). At zero weeks a correlation betwen the size of the pores and their density is observed in both ceramics ($p \leqslant 0.002$; $r \leqslant 0.913$). No correlation is found between the size and the interconnection density, nor between the interconnections and the pore size (Table V).

The microstructure of HA is not modified. On the other hand, for β-TCP, the peak of the interconnection distribution curve gradually flattens (Fig. 7). The mean size and density of the interconnections have significantly increased ($p < 0.05$) with time (Table V). At all times, the pore size correlates with pore density ($p < 0.02$; $r \leqslant 0.789$). After 12 weeks of implantation, a correlation between the densities of the interconnections and pores in β-TCP is seen ($p = 0.027$; $r = 0.765$). After 24 weeks there is also a significant correlation of interconnection sizes in relation to pore size ($p = 0.004$; $r = 0.88$) and pore density ($p = 0.021$; $r = -0.786$).

On stained sections, the size of interconnections containing chondroid tissue (14.136–47.78 μm) is smaller than interconnections containing bone tissue

TABLE III Cellular protein synthesis *in vitro*

Specimen ($n = 4$)	Type I procollagen (mcg/10^6 cells)		Osteocalcin (pM/10^6 cells)		Alkaline phosphatase (mU/10^6 cells) 21days of culture
	Vitamin D_3	Ethanol	Vitamin D_3	Ethanol	
HA	1.41 ± 0.21	1.31 ± 0.69	2.07 ± 0.45	0.37 ± 0.74	23.33 ± 15.34
β-TCP	1.82 ± 0.56	2.20 ± 0.56	–	–	26.14 ± 17.40

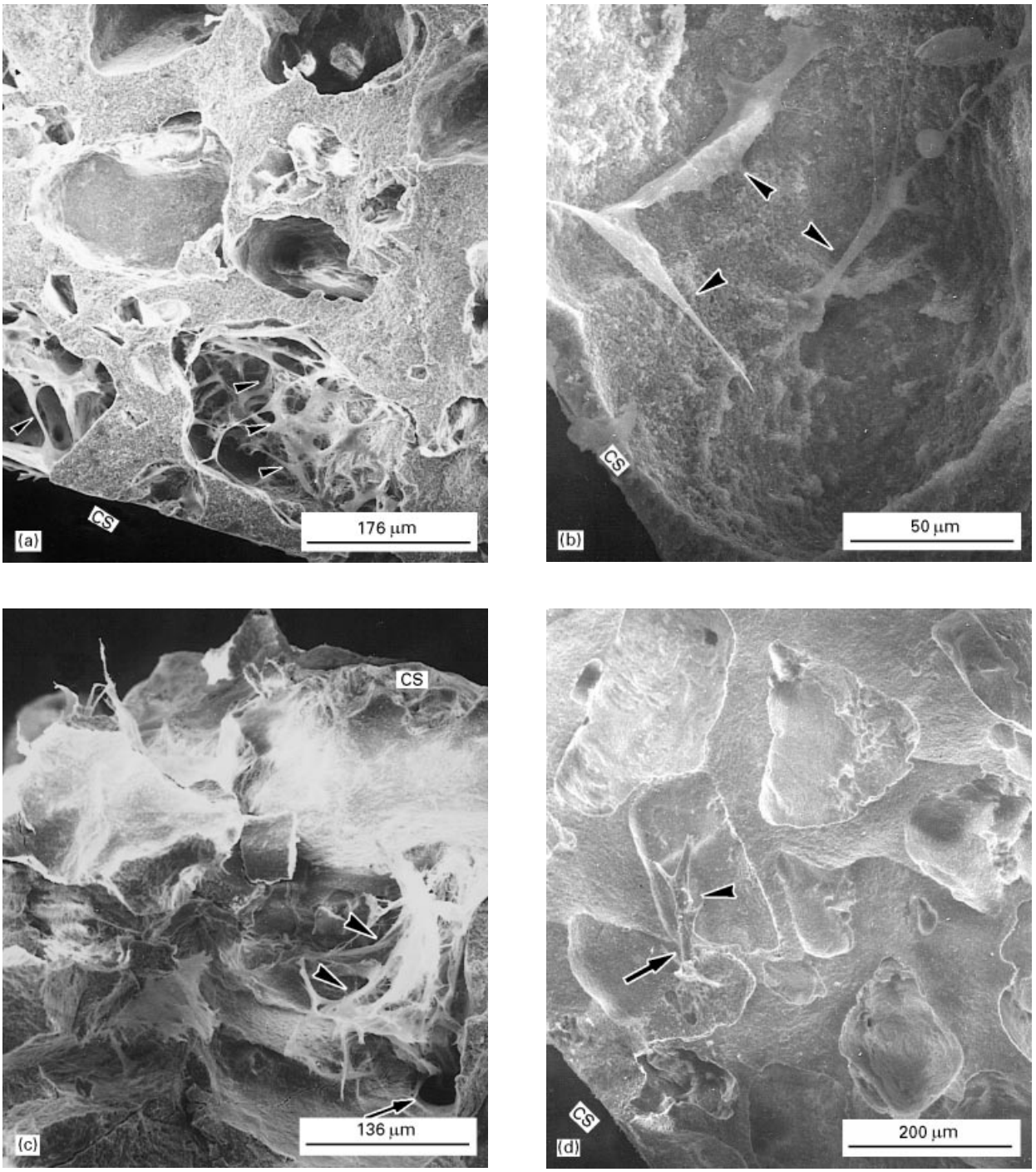

Figure 3 SEM, fracture surface of specimens *in vitro* (a, b) after 14 days of culture, and (c, d) after 28 days of culture. (a) β-TCP, showing numerous osteoblasts (short arrows) colonizing macropores near the contact surface (CS) between material–cells. (b) HA, showing a few osteoblasts (short arrows) located inside the pores near the CS. (c) β-TCP, showing osteoblasts (short arrows) going through the porous interconnection (long arrow). (d) HA, showing an osteoblast (short arrow) spreading across an interconnection (long arrow) and connecting two macropores.

(19.15–201.06 μm). These sizes were not significantly different with time (Table VI).

In β-TCP, after 12 weeks of implantation there is a correlation between bone formation and interconnection size ($p = 0.039$ $r = 0.733$) and between bone formation and pore density ($p = 0.037$; $r = -0.736$).

4. Discussion

The microstructure of porous materials, i.e. the volume, density and size of pores and interconnections and specific surface, acts on the degradation and bone ingrowth of materials. The effect of sizes on degradation and bone ingrowth have been widely investigated. Aside from chemical composition, biodegradation is directly influenced by pore size and volume [5]. An increase of porosity would favour bone ingrowth inside materials but would decrease their biomechanical properties. Then, some $50 \pm 5\%$ porosities have been used, many studies have focused on pore size [7]. White and Shors [8] consider that there is a relation between pore size and the tissue elements that favour good bone ingrowth: a pore size of 10 μm would allow ingrowth of cells, while a 15–50 μm pore size would

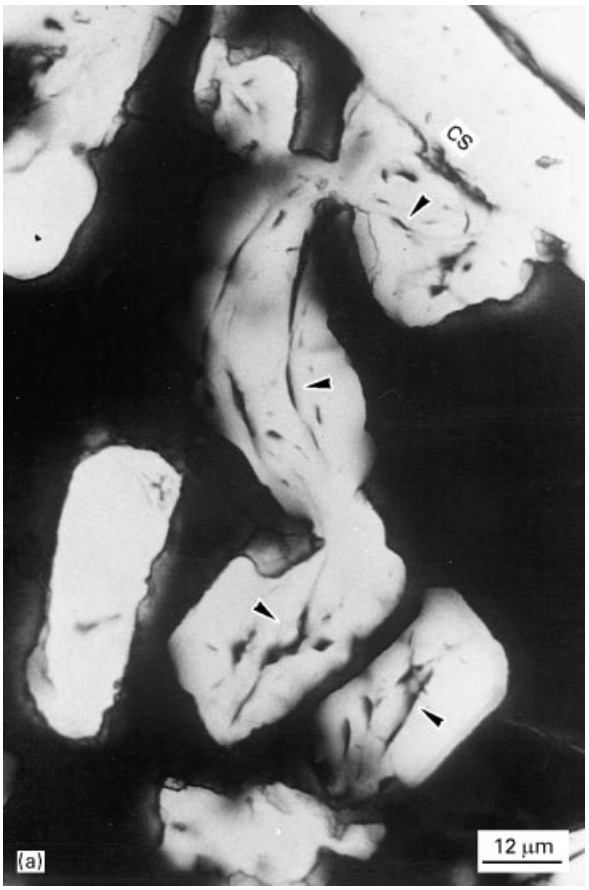

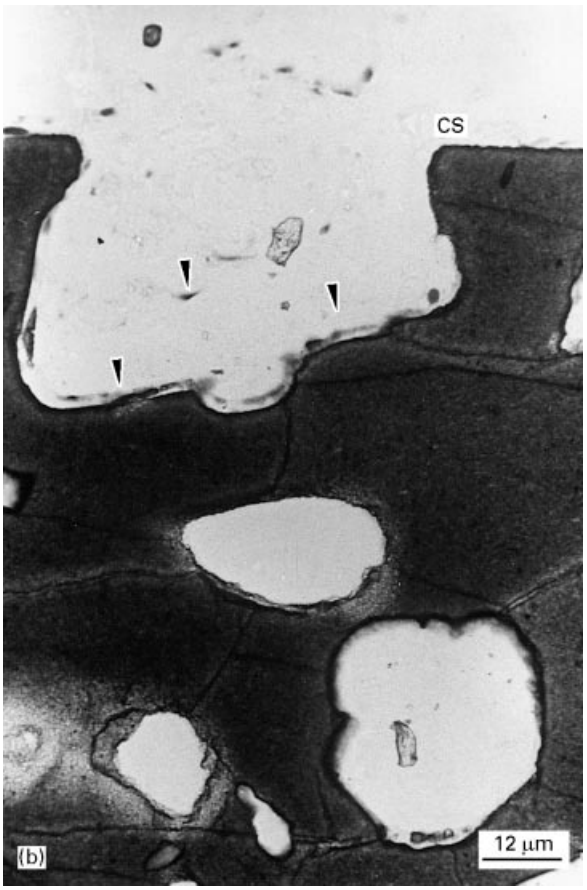

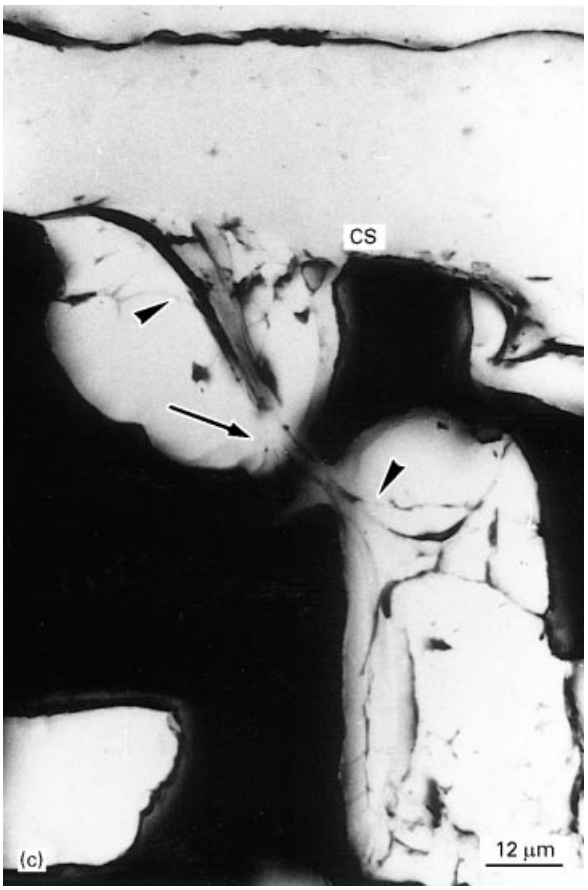

Figure 4 May Grünwald Giemsa stained section (50 μm thickness, Bar = 12 μm) showing the contact surface (CS) with osteoblasts after 14 days (a, b) and 28 days (c) of culture. (a) β-TCP, showing numerous osteoblasts (short arrows) covering the CS and having a depth penetration. (b) HA, showing a few osteoblasts (short arrows) covering the surface of the material without cellular penetration. (c) β-TCP, showing osteoblasts (short arrows) going through a 15 μm porous interconnection (long arrow).

assure fibrous tissue formation, and a pore size greater than 150 μm would favour new bone formation. However, the pore size for new bone formation is various in the reports. Eggli *et al.* [1] in a comparative study of β-TCP and HA have found that osteogenesis in the cortico-medullar site of the tibia in 50–100 μm pores is greater than in 200–400 μm size pores. On the other hand, Uchida *et al.* [5] have noticed that osteogenesis in HA, β-TCP and calcium aluminate (CA) was greater in 210–300 μm pores than in 150–210 μm pores. Kuhne *et al.* [2] have proved that osteogenesis in HA was higher in 500 μm pores than in 200 μm pores. However, these studies have neglected the effects of interconnections that influence directly the biological fluids, especially cells and vessels that favour tissue nutrition and condition new bone formation [9].

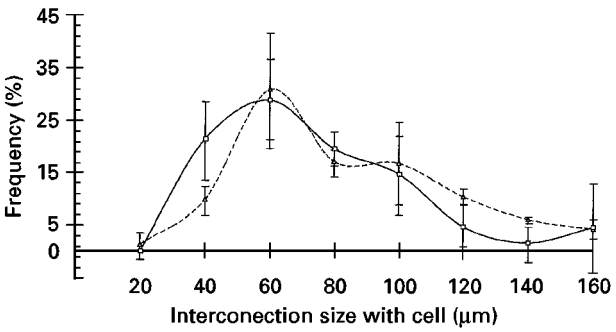

Figure 5 Distribution of interconnections with cells after 28 days *in vitro*: (——) TCP, (- - -) HA.

TABLE IV Histomorphometric parameters after implantation (n = 8)

Parameters	Groups	12 weeks	24 weeks
MAR, $\mu m\,d^{-1}$	HA	0.77 ± 0.10	0.77 ± 0.14
	β-TCP	0.91 ± 0.17 ($^{a}p = 0.000$)	1.25 ± 0.10 ($^{b}p = 0.000$, $^{a}p = 0.000$)
	Bone	1.81 ± 0.31	1.74 ± 0.20
PBTP, %	HA	29.85 ± 5.73	45.65 ± 10.46 ($^{b}p = 0.002$)
	β-TCP	100.00	100.00
PCTP, %	HA	56.53 ± 8.82	69.38 ± 8.78 ($^{b}p = 0.011$)
	β-TCP	—	—
NBV, %	HA	12.47 ± 3.19	14.18 ± 3.07
	β-TCP	35.00 ± 6.64 ($^{a}p = 0.000$)	52.07 ± 7.53 ($^{b}p = 0.035$, $^{a}p = 0.000$)
ROV, %	HA	14.43 ± 7.46	6.67 ± 3.08 ($^{b}p = 0.029$)
	β-TCP	7.48 ± 5.16 ($^{a}p = 0.007$)	3.42 ± 2.93 ($^{b}p = 0.035$, $^{a}p = 0.046$)
MDR, %	HA	3.41 ± 4.23	3.59 ± 4.96
	β-TCP	11.49 ± 7.66 ($^{a}p = 0.010$)	28.77 ± 12.9 ($^{b}p = 0.010$, $^{a}p = 0.002$)

[a] Comparison between materials.
[b] Comparison between times.

Galois *et al.* [10], who cultured rat fibroblasts on the surface of HA and β-TCP with different pore sizes, found no cells inside the ceramics after five and 40 days of culture. However, in our *in vitro* study, after embedding the discs with medium culture, the human osteoblasts crossed through 20 μm size interconnections, and spread and proliferated inside the macropores with time. However, the osteoblasts were seen only in the ring of ceramics (1.2 ± 0.2 mm), and never in the centre. To avoid the hydrophobic phenomenon of porous ceramics, air bubbles were extracted under vacuum favouring the medium penetration, and efficacy was justified using a medium with blue staining.

Shimazaki and Mooney [4] have compared 230 and 600 μm pore sizes, respectively, with 190 and 260 μm interconnections of HA in cortico-medullar of the rabbit femur. The results show bone ingrowth is higher for 600 μm than for 230 μm sized pores. In our

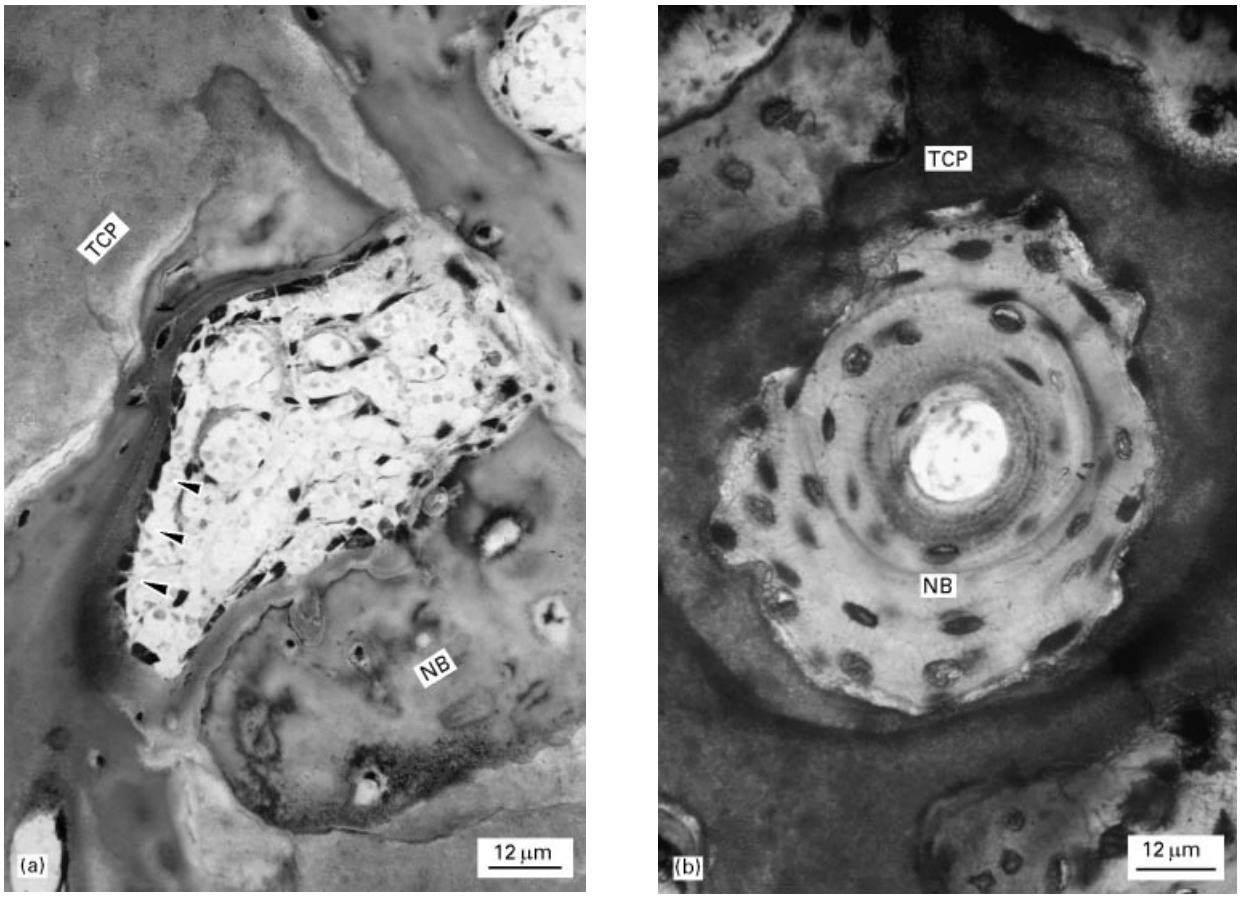

Figure 6 Van Gieson Picro-Fuschine stained section (50 μm thickness) (a, b) β-TCP after eight and 12 weeks of culture, respectively, and (c, d) HA after 24 and 12 weeks of culture, respectively. (a) β-TCP shows new bone (NB) formation with osteoid tissue and osteoblasts (short arrows) inside the pore. (b) NB formation inside the pore similar to Havers canal. (c) HA shows a good new bone–implant contact interface and fibrous bone penetration. Chondroid tissue (CT) is forming inside the macropores and passes through a < 15 μm porous interconnection (long arrow). (d) HA, showing CT and poor matrix mineralization.

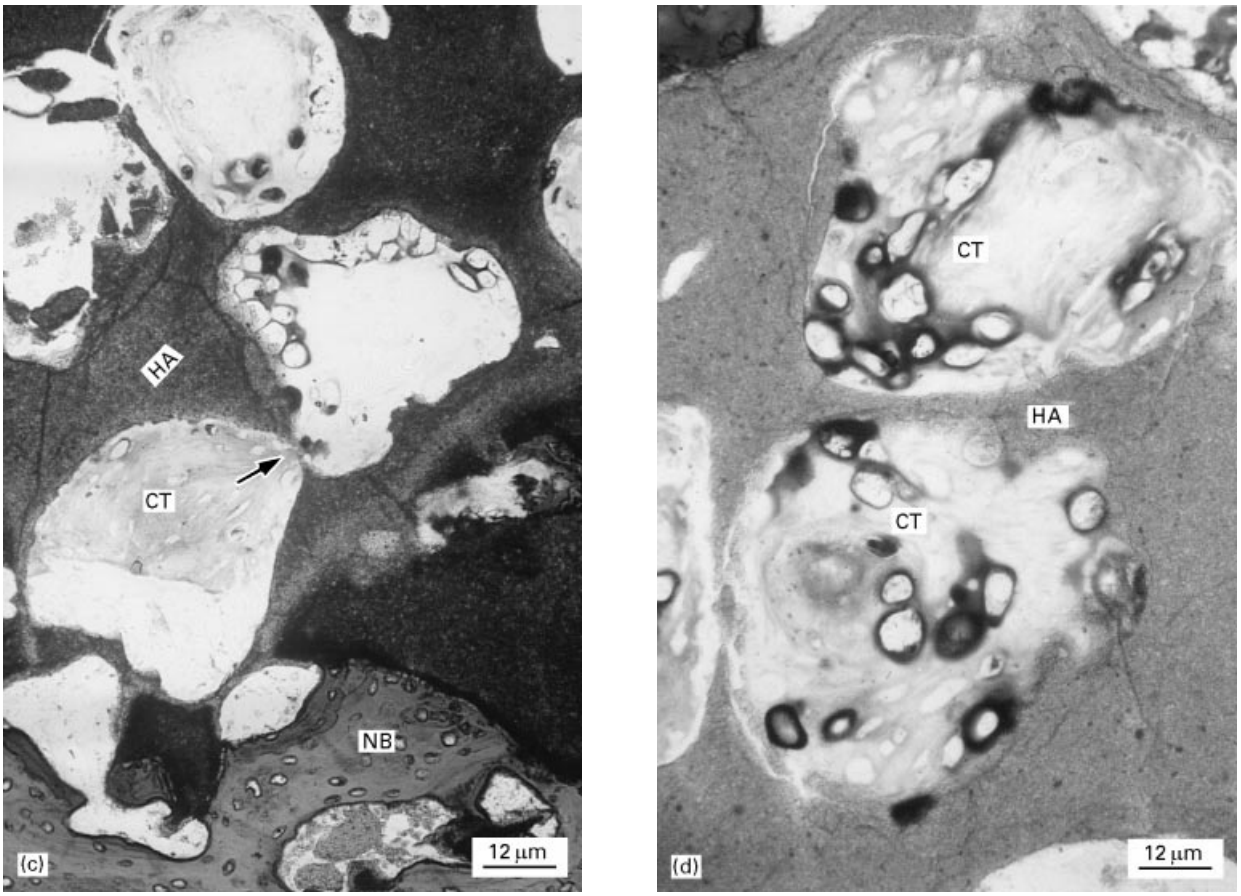

Figure 6 Continued.

TABLE V Characterization of the microstructure of biomaterials before and after implantation (n = 8)

	Time (weeks)	Macropores		Interconnections		Ratio IC/MP
		Size (μm)	Density (mm^2)	Size (μm)	Density (mm^2)	
HA	0	172.12 ± 9.41	22.06 ± 2.52	61.78 ± 5.75	10.13 ± 1.41	0.47 ± 0.04
β-TCP	0	165.62 ± 6.60	26.45 ± 1.90 [a]$p = 0.006$	63.93 ± 3.81	14.46 ± 1.67 [a]$p = 0.000$	0.55 ± 0.06 [a]$p = 0.007$
β-TCP	12	178.15 ± 11.56 [a]$p = 0.002$	21.72 ± 2.15 [b]$p = 0.001$	78.59 ± 5.21 [b]$p = 0.001$	17.58 ± 1.11 [b]$p = 0.013$	0.81 ± 0.05 [b]$p = 0.000$
β-TCP	24	202.63 ± 12.20 [b]$p = 0.011$	18.41 ± 1.77 [b]$p = 0.037$	93.83 ± 7.63 [b]$p = 0.006$	18.74 ± 2.49	1.02 ± 0.13 [b]$p = 0.002$

[a] Comparison between materials.
[b] Comparison between times.

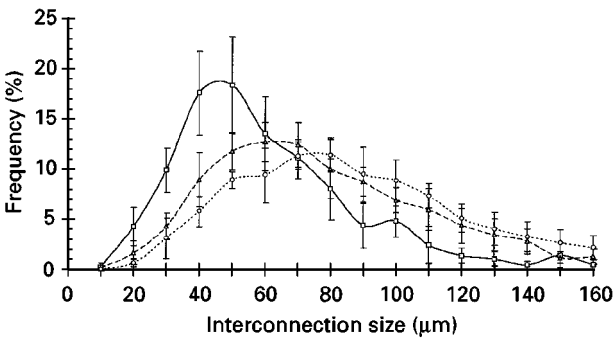

Figure 7 Distribution of β-TCP interconnections *in vivo* with time: (——) zero weeks, (- - -) 12 weeks, (· · · ·) 24 weeks.

TABLE VI Mean size (μm) of interconnections with a tissue (n = 8)

Time (weeks)	HA		β-TCP
	With chondroid tissue	With bone tissue	With bone tissue
12	26.21 ± 2.54	71.61 ± 4.95	74.40 ± 5.29
24	25.06 ± 1.32	68.27 ± 6.96	77.32 ± 5.47 [a]$p = 0.012$

[a] Comparison between materials.

results, the rate of calcification and bone ingrowth are not different with times in HA. Moreover, chondroid tissue increases with time ($p < 0.05$) and this increase is greater than new bone formation. A fibrillar bone tissue appears in 25 μm mean size interconnections because it allows only penetration of cells and insufficient supply of nutritional elements to favour new bone formation. In β-TCP, the rates of calcification and new bone formation increases significantly with time (Fig. 8a–d). At the same time, the size and density

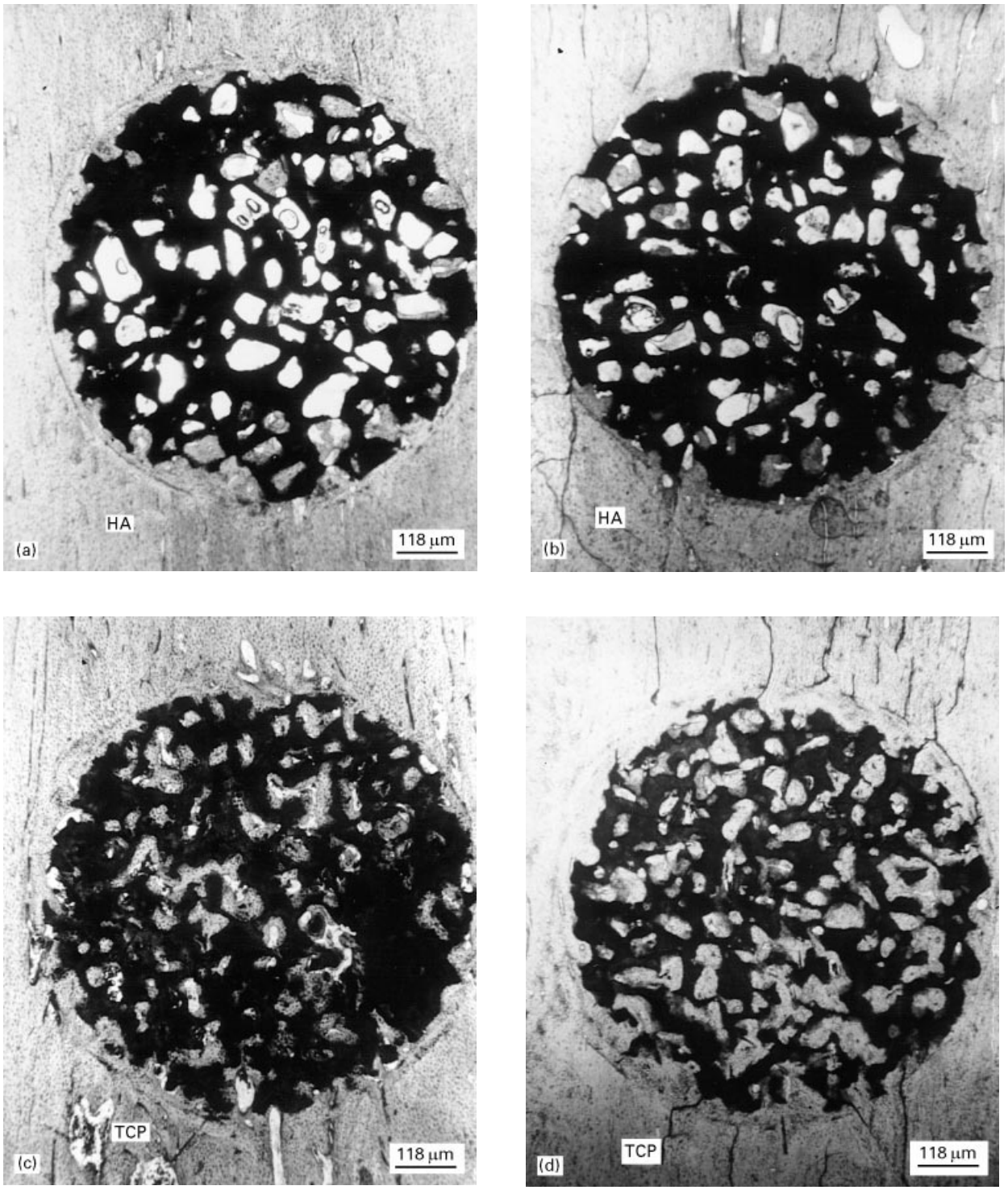

Figure 8 Van Gieson Picro-Fuschine stained section (50 μm thickness) showing the implant after implantation for (a, b) HA for 12 and 24 weeks, respectively (bone penetration remains in the periphery of the implant without material degradation), and (c, d) β-TCP for 12 and 24 weeks, respectively (there is good bone penetration in the whole implant with material degradation).

of interconnections in β-TCP increase with time. A correlation is observed between new bone formation and interconnection size or pore density after 12 weeks in β-TCP.

Klawitter and Hulbert [9] have noted that the size of interconnections in calcium aluminate should be at least 100 μm to favour mineralized bone tissue, 40–100 μm for osteoid tissue and 5–15 μm for fibrous tissue. White and Shors [8] consider that the size of interconnections must be over 100 μm. But, our results indicate that a size over 50 μm allows mineralized bone formation inside the macropores of the material. Indeed, we have measured the diameter of Volkman canals inside the ceramic microradiographically, these varied between 10 and 20 μm, with a high number have a diameter near 20 μm. Vascular penetration was deeper in β-TCP than in HA (Fig. 9a, b) because of the *in vivo* degradation of β-TCP. Interconnections act only as pathways for nutritional elements, vascularization and cells, although pores are the sites for bone tissue growth. Thus, pore size must be larger than interconnection size.

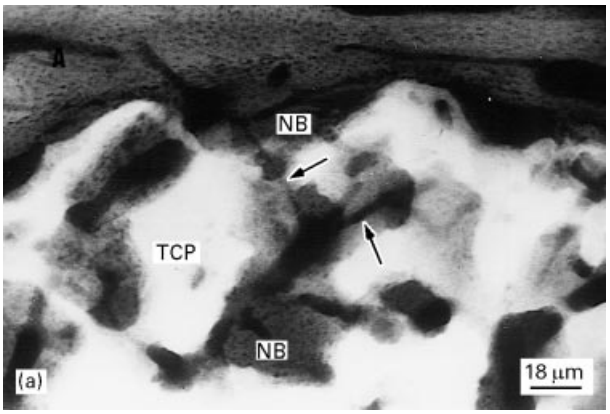

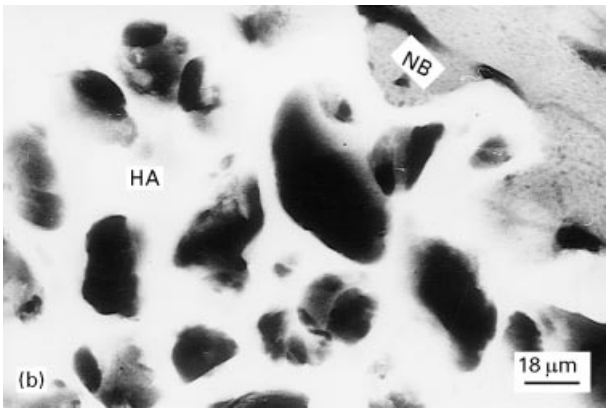

Figure 9 Microradiographs (100 μm thickness sections) showing β-TCP (a) and HA (b) after 12 weeks of implantation. (a) Volkman canals (long arrows) go through the interconnections and cross the implant; there is new bone (NB) formation inside the pores. (b) No vascular penetration or bone ingrowth inside pores (PM).

Before and after cell culture, we noticed that not only the size of the interconnections but also their density are important to favour cellular penetration inside porous ceramics. Our *in vitro* and *in vivo* investigations allow us to say that in resorbable materials, pore and interconnection densities play a more important role than their size, because sizes are modified by degradation. In unresorbable materials, there is a similar importance between the sizes and densities of both biomaterials.

5. Conclusions

The results presented in the present study clearly demonstrate that *in vitro*, human osteoblasts can cross through the interconnections, spread and proliferate inside macropores. The minimal necessary interconnection size is 20 μm, but the most favourable size for cell penetration is over 40 μm. *In vivo*, an interconnection size of over 20 μm permits cell penetration and chondroid tissue formation inside macropores. However, an interconnection size of over 50 μm can assure mineralized bone formation. Our results suggest that the density of interconnections plays an important role for bone formation.

Acknowledgements

We are grateful to Dr N. Guillemin for his advice and encouragement, to Mrs M. Bouville for technical assistance and to Mr R. Fromentin for help with the photography.

References

1. P. S. EGGLI, W. MÜLLER and R. K. SCHENK, *Clin. Orthop. Rel. Res.* **232** (1988) 127.
2. J. KÜHNE, R. BARTL, B. FRISCH, C. HAMMER, V. JANSSON and M. ZIMMER, *Acta Orthop. Scand.* **65** (1994) 246.
3. A. UCHIDA, S. NADE, E. McCARTNEY and W. CHING, *J. Orthop. Res.* **3** (1985) 65.
4. K. SHIMAZAKI and V. MOONEY, *ibid.* **3** (1985) 301.
5. A. UCHIDA, S. M. L. NADE, E. R. McCARTNEY and W. CHING, *J. Bone Joint Surg.* **66B** (1984) 269.
6. A. M. PARFITT, M. K. DREZNER, F. H. GLORIEUX, J. A. KANIS, H. MALLUCHE, P. J. MEUNIER and S. M. OTT, *J. Bone Min. Res.* **2** (1987) 595.
7. R. Z. LE GEROS, J. R. PARSONS, G. DACULSI, F. DRISSENS, D. LEE, S. T. LIU, D. PETERSON and M. WALKER, *New York Acad. Sci.* **523** (1988) 268.
8. E. WHITE and E. C. SHORS, *Dent. Clin. N. Amer.* **30** (1986) 49.
9. J. J. KLAWITTER and S. F. HULBERT, *J. Biomed. Mater. Res. Symp.* **2** (1971) 161.
10. L. GALOIS, D. MAINARD, K. BORDJI, H. MEMBRE, L. MARCHAL, B. FOLIQUET, D. CLEMENT and J. P. DELAGOUTTE, in *Actualités en matériau* **3** (1990) 361.

Received 26 March 1997
and accepted 26 January 1998